

Antibacterial activity assays of a new cadmium complex with o-phenanthroline and cyanoguanidine: crystal structure, fluorescence properties, and chemical speciation studies

LEONOR L. LÓPEZ TÉVEZ[†], JUAN J. MARTÍNEZ MEDINA[†],
MARÍA S. ISLAS[‡], OSCAR E. PIRO[§], EDUARDO E. CASTELLANO[¶],
LILIANA BRUZZONE[⊥], EVELINA G. FERRER[‡] and
PATRICIA A.M. WILLIAMS^{*‡}

[†]Departamento de Química, UNCAUS, Cte. Fernández 755 (3700),
Chaco, Argentina

[‡]Centro de Química Inorgánica (CEQUINOR), FCE, UNLP, 47 y 115 (1900)
La Plata, Argentina

[§]Instituto IFLP (CONICET-CCT La Plata) y Departamento de Física, Facultad de Ciencias
Exactas (FCE), UNLP, 49 y 115 (1900) La Plata, Argentina

[¶]Instituto de Física de São Carlos, Universidade de São Paulo, C.P. 369,
13560 São Carlos (SP), Brazil

[⊥]División Química Analítica, FCE, UNLP, 47 y 115 (1900) La Plata, Argentina

(Received 15 July 2011; in final form 2 September 2011)

A new coordination complex, aqua bis(o-phenanthroline) cadmium(II) sulfate cyanoguanidine pentahydrate, $[\text{Cd}(\text{o-phen})_2(\text{SO}_4)(\text{H}_2\text{O})](\text{cng}) \cdot 5\text{H}_2\text{O}$, was synthesized and characterized. The crystal structure was solved by X-ray diffraction methods. It crystallizes in the monoclinic space group $P2_1/n$ with $a = 13.7650(2)$ Å, $b = 10.2796(2)$ Å, $c = 21.4418(3)$ Å, $\beta = 90.106(2)^\circ$, and $Z = 4$ molecules per cell unit. The cadmium(II) is in a distorted octahedral environment coordinated to two nearly planar and mutually perpendicular o-phenanthrolines, one oxygen atom of sulfate, and a water molecule. Non-bonded and planar cyanoguanidine and five crystallization water molecules complete the asymmetric unit. Vibrational (FT-IR and FT-Raman) spectroscopies and thermogravimetric determinations support this structure. Intensity enhancement of the fluorescence spectrum may be a demonstration of the interaction of the metal with phenanthroline. In solution the coordination behavior is rather different, and the speciation studies point to coordination of both cng and phenanthroline to cadmium. The improvement of the antibacterial activity of cadmium upon complexation has been determined.

Keywords: Phenanthroline; Cyanoguanidine; Cadmium complexes; Crystal structure; Antibacterial properties

1. Introduction

Complexation of cadmium with ligands that mimic naturally occurring compounds could be a new and useful therapy to treatment of malignancies. Cadmium was

*Corresponding author. Email: williams@quimica.unlp.edu.ar

designated as a human carcinogen by the International Agency for Research on Cancer due to the known toxicity [1, 2]. Nevertheless, it has been demonstrated that cadmium toxicity depends on the salt used and that toxicity can be modulated by complexation. For instance, Cd(II) 1,10-phenanthroline complexes strongly interact with DNA and the affinity of the bonding with nucleic bases decreases in the presence of EDTA or citric acid [3], acyclic nucleotide Cd(II) complexes are active against a variety of viruses [4], Cd(II) complexes containing the CdN₆ core showed significant inhibitory activity on glioma cells [5] and cadmium thiocarbodiazone derivatives behave as cytotoxic agents capable of improving antitumor activity in cisplatin-resistant tumors [6]. As a part of a series of studies involving metal coordination complexes with potential biological activities, the antibacterial properties of a new cadmium complex are evaluated with Gram negative and Gram positive strains; the general effect is the improvement of the activity on metal complexation. In this communication the synthesis, characterization and structural determination of a complex with a CdO₂N₄ core formed between Cd(SO₄), phenanthroline and cyanoguanidine is reported. Cyanoguanidine does not bond to Cd(II), but is attached to the complex by H-bonding to the water and sulfate. Speciation in aqueous solution shows that the major species at physiological pH values is a ternary complex in which the cadmium(II) is linked to two phenanthroline ligands and one cyanoguanidine.

2. Experimental

2.1. Reagents and instrumentation

All chemicals were of analytical grade and used without purification. Cadmium sulfate octahydrate was purchased from Alfa Chemicals and cyanoguanidine and o-phenanthroline from Sigma.

FTIR spectra of powdered samples were measured with a Bruker IFS 66 FTIR-spectrophotometer from 4000 to 400 cm⁻¹ as KBr pellets. Raman spectra were obtained with a fast Fourier transform FRA106 Bruker spectrometer using the 1064 nm line of an Nd-YAG ion laser for excitation. Elemental analyses for carbon, hydrogen, and nitrogen were performed using a Carlo Erba EA 1108 analyzer. Thermogravimetric (TG) and differential thermal analyses (DTA) were performed on a Shimadzu system (models TG-50 and DTA-50, respectively), working in an oxygen flow (50 mL min⁻¹) and at a heating rate of 10°C min⁻¹. Sample quantities ranged between 10 and 20 mg. Al₂O₃ was used as a DTA standard. Fluorescence measurements were carried out on a Perkin-Elmer LS-50B luminescence spectrometer (Beaconsfield, England) equipped with a quartz cell of 1 cm path length, a pulsed xenon lamp (half peak height < 10 μs, 60 Hz), an R928 photomultiplier tube, and a computer working with FL Winlab software. Both excitation and emission slits were 10 nm.

2.2. Antibacterial assay

The antibacterial activities of cadmium, phenanthroline, cyanoguanidine, and the ternary complex have been investigated against four strains of bacteria (*Escherichia coli* (ATCC 35218), *Staphylococcus aureus* (ATCC 25923), *Pseudomonas aeruginosa*

(ATCC 27853), and *Enterococcus faecalis* (ATCC 29212)) by the disc diffusion method. The sensitivities of the metals and ligands were tested using Mueller–Hinton (MH) agar plates.

The microorganisms were transferred to separate test tubes containing 15 mL of a sterile MH broth and incubated for 18 h at 35–37°C. Sufficient inoculums were added in new tubes until the turbidity equaled 0.5 McFarland (approximately 10^8 colony-forming unit per mL, CFU per mL). The bacterial inoculums diluted with MH broth (McFarland standard) were uniformly spread using sterile cotton swabs on sterile Petri dishes MH agar. Aqueous (0.10 mol L^{-1}) solutions of cadmium chloride, phenanthroline, cyanoguanidine, and the complex were prepared, autoclaved, and cooled. Sterile filter paper discs of 6 mm in diameter were aseptically impregnated with the sterile solutions of the compounds. All impregnated discs were allowed to stand until complete solvent evaporation and placed on the surface of previously inoculated solid agar. The discs were then wetted with 40 μL of a solution of each compound to be tested, in a concentration of 100 mmol L^{-1} in DMSO/water. The plates were incubated for 18 h at 35–37 °C and examined thereafter. Clear zones of inhibition formed around the discs were observed and the compound sensitivity was assayed from the measurement of the diameter of inhibition (in mm) [7–9]. Values reported are an average of at least three independent experiments.

2.3. Syntheses

2.3.1. $[\text{Cd}(\text{o-phen})_2(\text{SO}_4)(\text{H}_2\text{O})](\text{cnge}) \cdot 5\text{H}_2\text{O}$. To an aqueous solution of $\text{CdSO}_4 \cdot 8\text{H}_2\text{O}$ (1 mmol), solutions of phenanthroline (in ethanol) and cyanoguanidine (in water) were added in a ratio 1 : 2 : 1. The pH of the suspension was raised to 10 using 1 mol L^{-1} NaOH. The precipitate that formed immediately was discarded and the mother liquor was left to evaporate at room temperature. Crystals adequate for crystallographic studies were obtained after 1 week. The crystals were washed with water and air dried. Anal. Calcd for $\text{C}_{26}\text{H}_{32}\text{N}_8\text{SO}_{10}\text{Cd}$ (%): C, 41.1; H, 4.2; N, 14.7. Found: C, 41.2; H, 4.1; N, 14.7.

2.4. Crystal structure determination

Measurements were performed on an Enraf-Nonius Kappa-CCD diffractometer with graphite-monochromated Mo-K α ($\lambda = 0.71073 \text{ \AA}$) radiation. Low-temperature diffraction data were collected (ϕ and ω scans with κ -offsets) with COLLECT [10]. Integration and scaling of the reflections were performed with the HKL DENZO-SCALEPACK [11] suite of programs. Unit cell parameters were obtained by least-squares refinement based on the angular settings for all collected reflections using HKL SCALEPACK [11]. The structure was solved by direct methods with SHELXS-97 [12] and the molecular model refined by full-matrix least-squares procedure on F^2 with SHELXL-97 [13]. Hydrogen atoms of o-phenanthroline (o-phen) and cyanoguanidine (cnge) were positioned stereochemically and refined with the riding model. The water hydrogen atoms were found in a difference Fourier map and refined with the Ow–H distances constrained to a target value of $0.84(1) \text{ \AA}$ and an isotropic displacement

parameter equal to 1.5 times the value of the corresponding oxygen. Crystal data and refinement results are summarized in table 1.

2.5. Potentiometric titrations

Potentiometric titrations were performed using 25 mL aliquots. NaCl (Merck p.a.) was dried until constant weight and then stored in a desiccator. The solids were dissolved in boiled triply distilled water and then cooled under constant nitrogen flow. Solutions were freshly prepared prior to their use. Diluted solutions of HCl (Merck p.a.) were standardized against TRISMA-base (hydroxymethyl aminomethane). Diluted NaOH solutions were prepared from a saturated NaOH solution and standardized against HCl. To assess the degree of carbonate contamination, the method of Gran was used [14]. The ionic strength was fixed at 0.150 mol L^{-1} with NaCl in the solutions and the temperature was kept at $25 \pm 0.1^\circ\text{C}$. The glass electrode was calibrated by titration of a known concentration of a solution of HCl with a standard base solution. It was checked separately in a solution with known $[\text{H}^+]$ before and after each titration.

The formation constants denoted β_{pqrs} corresponds to the general notation:



Table 1. Crystal data and structure refinement for $[\text{Cd}(\text{o-phen})_2(\text{SO}_4)(\text{H}_2\text{O})](\text{cnge}) \cdot 5\text{H}_2\text{O}$.

Empirical formula	$\text{C}_{26}\text{H}_{32}\text{CdN}_8\text{O}_{10}\text{S}$
Formula weight	761.06
Temperature (K)	100(2)
Wavelength (\AA)	0.71073
Crystal system	Monoclinic
Space group	$P2_1/n$
Unit cell dimensions (\AA , $^\circ$)	
<i>a</i>	13.7650(2)
<i>b</i>	10.2796(2)
<i>c</i>	21.4418(3)
β	90.106(2)
Volume (\AA^3), <i>Z</i>	3033.98(9), 4
Calculated density (Mg m^{-3})	1.666
Absorption coefficient (mm^{-1})	0.859
<i>F</i> (000)	1552
Crystal size (mm^3)	$0.23 \times 0.18 \times 0.14$
θ range for data collection ($^\circ$)	2.96–26.00
Index ranges	$-16 \leq h \leq 16$; $-12 \leq k \leq 11$; $-25 \leq l \leq 25$
Reflections collected/unique	32,141/5710 [$R(\text{int}) = 0.039$]
Observed reflections [$I > 2\sigma(I)$]	4939
Completeness to $\theta = 26.00$ (%)	95.8
Refinement method	Full-matrix least-squares on F^2
Weights, <i>w</i>	$[\sigma^2(F_o^2) + (0.0362 P)^2 + 2.33 P]^{-1}$ $P = [\max(F_o^2, 0) + 2F_c^2]/3$
Data/restraints/parameters	5710/12/452
Goodness-of-fit on F^2	1.037
Final <i>R</i> indices [$I > 2\sigma(I)$] ^a	$R_1 = 0.0262$, $wR_2 = 0.0641$
<i>R</i> indices (all data)	$R_1 = 0.0342$, $wR_2 = 0.0681$
Largest difference peak and hole (e \AA^{-3})	0.548 and -0.970

^a $R_1 = \sum ||F_o| - |F_c|| / \sum |F_o|$; $wR_2 = [\sum w(|F_o|^2 - |F_c|^2)^2 / \sum w(|F_o|^2)^2]^{1/2}$.

A value of $pK_w = 13.76$ (corresponding to $\log \beta_{000-1} = -13.76$) was assumed for the experimental conditions ($T = 298 \text{ K}$, $I = 150 \text{ mmol L}^{-1}$, nitrogen atmosphere). The determined dissociation constants (pK_a) for cngeH [15], phenH^+ , and the formation constants for the ternary system $\text{Cd}^{2+}/\text{phen}/\text{H}^+$ have been previously determined, and our data were in good agreement with these values [16–19].

To determine the formation constants of the $\text{Cd}^{2+}/\text{cnge}/\text{H}^+$ system, four sets of titrations were performed from pH 2–10. Total concentration of cadmium in the vessel was 0.1 mmol L^{-1} and the metal/ligand ratio was 1/2. Four titrations of these solutions were performed on the $\text{Cd}^{2+}/\text{phen}/\text{cnge}/\text{H}^+$ system. $\text{Cd}^{2+}/\text{phen}/\text{cnge}$ concentrations were $0.5 \text{ mmol L}^{-1}/1.5 \text{ mmol L}^{-1}/1 \text{ mmol L}^{-1}$ and the pH ranged from 2 to 11.

3. Results and discussion

3.1. Structural description

Atomic fractional coordinates and equivalent isotropic displacement parameters are shown in table S1. Intramolecular bond distances and angles within the cyanoguanidine molecule and around cadmium(II) are shown in table 2. Figure 1 is an ORTEP [20] drawing of the complex.

The cadmium(II) is in a distorted octahedral environment coordinated to two nearly planar (*rms* deviation of atoms from the best least-squares plane was less than 0.06 \AA) and mutually perpendicular *o*-phenanthrolines (dihedral angle of $77.35(3)^\circ$; Cd–N bond lengths ranging from $2.336(2)$ to $2.383(2) \text{ \AA}$). These values are in good agreement with those found in other Cd-phenanthroline complexes [21–25].

The remaining two *cis*-positions are occupied by one oxygen atom of a sulfate [$d(\text{Cd}-\text{O}) = 2.269(1) \text{ \AA}$] and a water molecule [$d(\text{Cd}-\text{Ow}) = 2.311(2) \text{ \AA}$]. A non-coordinated cyanoguanidine (*rms* deviation of atoms from molecular plane of 0.015 \AA) and five crystallization water molecules complete the asymmetric unit. The crystal is further stabilized by an extended H-bonding network where the water molecules are donors in $\text{Ow}-\text{H}\cdots\text{Ow}$ [$d(\text{Ow}\cdots\text{Ow})$: 2.691 – 2.963 \AA and $\angle(\text{Ow}-\text{H}\cdots\text{Ow})$: 146.0 – 178.4°], $\text{Ow}-\text{H}\cdots\text{O}(\text{sulf})$ [$d(\text{Ow}\cdots\text{O})$: 2.784 – 2.938 \AA and $\angle(\text{Ow}-\text{H}\cdots\text{O})$: 151.5 – 171.7°], and $\text{Ow}-\text{H}\cdots\text{N}(\text{cnge})$ [$d(\text{Ow}\cdots\text{N})$: 2.891 and 2.877 \AA and $\angle(\text{Ow}-\text{H}\cdots\text{N})$: 166.7 and 159.9° , respectively] interactions. The cyanoguanidine also is a donor in further H-bonds involving their NH_2 groups in three $\text{N}-\text{H}\cdots\text{O}(\text{sulf})$ interactions [$d(\text{N}\cdots\text{O})$: 2.890 – 2.985 \AA and $\angle(\text{N}-\text{H}\cdots\text{O})$: 158.3 – 166.7°] and one $\text{N}-\text{H}\cdots\text{Ow}$ bond [$d(\text{N}\cdots\text{Ow}) = 2.963 \text{ \AA}$ and $\angle(\text{N}-\text{H}\cdots\text{Ow}) = 146.0^\circ$]. Full detail of the H-bonding structure is provided as “Supplementary material.” The presence of cyanoguanidine avoids catena complex formations in which the sulfates are linkers between the metal centers [26].

3.2. Thermal behavior

The TG trace is characterized by five weight losses to 700°C . The first of 12.0% at 100°C is due to loss of five hydration water molecules (expected 11.8%). This process is accompanied by a weak endothermic DTA signal at 78.5°C typical of water release. After release of water, a complex degradation process of the remaining material is

Table 2. Intramolecular bond distances (Å) and angles (°) in the cyanoguanidine and around cadmium(II) in $[\text{Cd}(\text{o-phen})_2(\text{SO}_4)(\text{H}_2\text{O})](\text{cnge}) \cdot 5\text{H}_2\text{O}$.

N(1)–C(2)	1.307(3)
N(1)–C(1)	1.344(3)
N(2)–C(2)	1.165(3)
N(3)–C(1)	1.333(3)
N(4)–C(1)	1.327(3)
Cd–O(31)	2.269(1)
Cd–O(1W)	2.311(2)
Cd–N(12)	2.336(2)
Cd–N(11)	2.339(2)
Cd–N(22)	2.340(2)
Cd–N(21)	2.383(2)
C(2)–N(1)–C(1)	118.9(2)
N(4)–C(1)–N(3)	119.4(2)
N(4)–C(1)–N(1)	117.1(2)
N(3)–C(1)–N(1)	123.6(2)
N(2)–C(2)–N(1)	172.7(2)
O(31)–Cd–O(1W)	84.81(5)
O(31)–Cd–N(12)	89.15(6)
O(1W)–Cd–N(12)	116.57(6)
O(31)–Cd–N(11)	157.57(6)
O(1W)–Cd–N(11)	93.21(6)
N(12)–Cd–N(11)	71.73(6)
O(31)–Cd–N(22)	107.09(6)
O(1W)–Cd–N(22)	86.66(6)
N(12)–Cd–N(22)	153.20(6)
N(11)–Cd–N(22)	95.07(6)
O(31)–Cd–N(21)	88.59(5)
O(1W)–Cd–N(21)	153.84(6)
N(12)–Cd–N(21)	88.55(6)
N(11)–Cd–N(21)	102.16(6)
N(22)–Cd–N(21)	71.14(6)

observed, due to loss of linked water and ligands and result in CdO at 600°C (experimental residue, 17.0%; theoretical residue, 16.9%). The characterization of CdO has been performed by FTIR spectroscopy [27].

3.3. Vibrational spectra

In table 3, assignments of vibration modes of each ligand and Cd complex are shown. Main bands of the Raman spectra are shown in italics. Typical phenanthroline bands are observed split and shifted hence indicating ligand–metal interaction. The doublet in the CN stretching region of cyanoguanidine (*ca* 2200 cm^{-1}), with the low-frequency component more intense than the high-frequency one in Raman spectra, is due to the presence of tautomeric forms [28] and the amino- or imino-tautomer formation is solvent-dependent [29]; this doublet is sensitive to coordination to transition metals. The spectral shift of this mode depends on the metal–N(cnge) distance [15]. This mode appears nearly at the same position upon complexation, therefore it is inferred that cnge is not coordinated to the cadmium in the complex, in accord with the X-ray diffraction data. The small blue shift observed for these bands in the complex could be assigned to

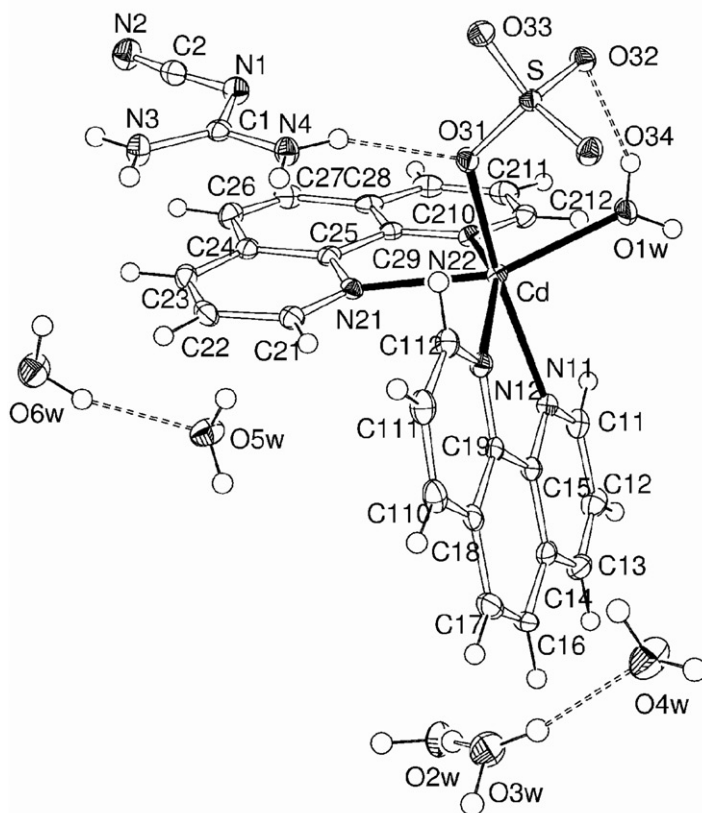


Figure 1. View of $[\text{Cd}(\text{o-phen})_2(\text{SO}_4)(\text{H}_2\text{O})](\text{cng}) \cdot 5\text{H}_2\text{O}$ in the solid showing labels of non-H atoms and their displacement ellipsoids at the 50% probability level. Cadmium-ligand bonds are indicated by full lines. For clarity, only a few representative H-bonds (in dashed lines) have been included in the plot.

H-bond formation (see “Supplementary material”). This is confirmed by observed weakening of the Raman dispersion at 930 cm^{-1} , due to the strongly active symmetric CN stretching mode of cng. The C=N double bond vibrations are at $1550\text{--}1580\text{ cm}^{-1}$ and bands due to deformation vibrations of NH of the amino tautomer (1505 cm^{-1}) are overlapped with o-phen bands.

When the sulfate (T_d symmetry) coordinates as a monodentate ligand, the symmetry diminishes to C_{3v} . In this case, ν_3 and ν_4 split and ν_1 and ν_2 modes (Raman active) became infrared (IR) active. The strong IR bands assigned to ν_3 and ν_4 modes (antisymmetric stretchings) appeared as weak bands in the Raman spectra. The observed bands corresponding to ν_1 and ν_2 retain their intensity in both FTIR and Raman spectra. Coordination of sulfate through one oxygen atom with C_{3v} symmetry is then assumed based on vibration spectroscopy (see table 3) [30] and confirmed by X-ray determinations.

Table 3. Wavenumbers (cm^{-1}) and proposed assignment of the FTIR and Raman (italics) spectra of $[\text{Cd}(\text{phen})_2(\text{H}_2\text{O})\text{SO}_4] \cdot (\text{cnge}) \cdot 5\text{H}_2\text{O}$, cyanoguanidine, and phenanthroline.

$[\text{Cd}(\text{phen})_2(\text{H}_2\text{O})\text{SO}_4] \cdot (\text{cnge}) \cdot 5\text{H}_2\text{O}$	cnge	phen	Assignments
2201 m	2208 m		$\nu(\text{C}\equiv\text{N})$ cnge
<i>2195 mw</i>	<i>2204 m</i>		
2156 s	2162 s		$\nu(\text{C}\equiv\text{N})$ cnge
<i>2156 m</i>	<i>2158 vs</i>		
1672 sh, 1634 s, 1621 sh	1637 ms	1645 m, 1620 w	
<i>1622 m</i>	<i>1647 w, 1635 w</i>	<i>1617 w</i>	
1594 m		1585 m	o-phen
<i>1604 m, 1592 m, 1580 sh</i>		<i>1601 w, 1590 w</i>	
1554 vs, 1547 vs	1570 s	1558 m	
	<i>1543 w</i>	<i>1564 vw</i>	
1514 vs, 1496 sh	1505 m	1501 s	
<i>1515 m</i>	<i>1524 w</i>	<i>1503 w</i>	
1425 s		1418 s	o-phen
<i>1450 m, 1412 vs</i>		<i>1447 m, 1405 vs</i>	
1345 m		1341 m	o-phen
<i>1345 w</i>		<i>1345 w</i>	
<i>1303 m</i>		1297 w	o-phen
		<i>1295 m</i>	
1257 m	1252 m	<i>1273 w</i>	
1224 m		1215 w	o-phen
		1183 w	o-phen
1148 s, 1104 s			ν_3 O-SO ₃
<i>1103 w</i>			
	1086 m	1090 m	
	<i>1098 w</i>	1090 w	ν_3 O-SO ₃
1061 vs			
<i>1052 m</i>			
		1034 w	o-phen
		<i>1036 m</i>	
		990 w	ν_1 O-SO ₃
976 m			
<i>974 m</i>			
		961 w	o-phen
934 m	928 m		$\nu_s(\text{C}\equiv\text{N})$ cnge
<i>928 w</i>	<i>934 s</i>		
862 m, 849 m		852 vs	o-phen
<i>864 w</i>			
773 m, 760 sh		776 w	o-phen
<i>727 m</i>	723 w	738 vs	o-phen
<i>725 m</i>		<i>711 m</i>	
666 m	671 m	693 m	
<i>667 vw</i>	<i>667 m</i>		
624 m		617 m	ν_4 O-SO ₃
<i>636 vw, 605 vw</i>			
<i>556 w</i>	555 m	584 w, 564 w	
		<i>551 w</i>	
521 m	521 m		cnge
<i>510 vw</i>	<i>519 m</i>		
497 m	498 m	500 m	
<i>497 vw</i>			
<i>470 vw</i>	465 m	448 w	
432 w			
419 m			ν_2 O-SO ₃
<i>421 m</i>			
407 w		410 w	

s, strong; m, medium; w, weak; sh, shoulder.

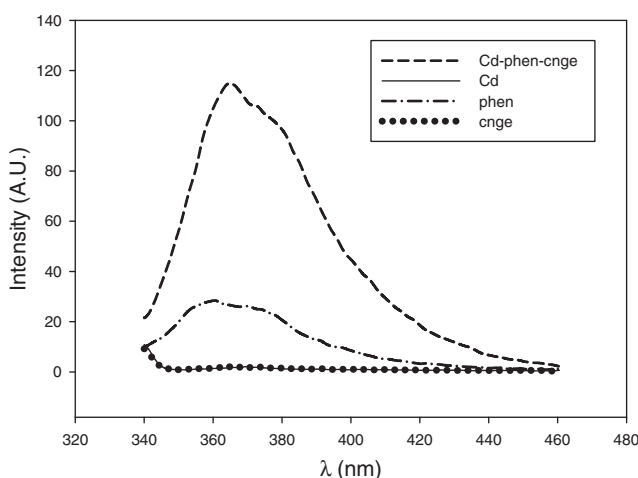


Figure 2. Fluorescence emission spectra of $[\text{Cd}(\text{o-phen})_2(\text{SO}_4)](\text{cnge}) \cdot 5\text{H}_2\text{O}$ and its components in a water–ethanol 1:1 mixture. Species concentrations are $1 \times 10^{-3} \text{ mol L}^{-1}$, except phenanthroline ($2 \times 10^{-3} \text{ mol L}^{-1}$), at room temperature.

3.4. Fluorescence spectra

Taking into account the excellent fluorescence properties of metal complexes with d^{10} configuration, the fluorescence spectra of the complex, the metal, and the ligands were measured in a mixture 1:1 of water–ethanol. Upon excitation of phenanthroline at 327 nm, emission bands at 365 nm and 388 nm were observed, which correspond to $\pi \rightarrow \pi^*$ transition. The complex shows an increase in the fluorescence intensity when compared with the ligand (figure 2). In this context, the spectrum band emission of the Cd complex can also be assigned to intraligand transitions. The intensity enhancement may be due to ligand coordination to the metal center, which increases the conformational rigidity of the ligand, thereby reducing the non-radiative decay of the intraligand $\pi \rightarrow \pi^*$ excited state [31, 32].

3.5. Stability constants

To get a better understanding of the behavior of the system in solution and to identify the nature of the bioactive species which is likely to interact with bacteria, potentiometric titration studies were undertaken. The ligand deprotonation constants were recalculated by means of potentiometric measurements from different sets of titrations using the Best program [33]. As stated in the experimental part, the calculated data of cyanoguanidine (LH, cngeH : $\text{p}K = 11.57$) and phenanthroline (AH^+ , phenH^+ : $\text{p}K = 5.00$) are in agreement with reported data (tables 4 and 5).

To determine the formation constants of the ternary ($\text{Cd}^{2+}/\text{cngeH}/\text{H}^+$ and $\text{Cd}^{2+}/\text{phen}/\text{H}^+$) and quaternary ($\text{Cd}^{2+}/\text{phen}/\text{cngeH}/\text{H}^+$) systems, data collected from several sets of titrations were analyzed with Best and Superquad calculation programs. The usual criteria for this kind of program (CHI^2 , R values, standard deviations, etc.) were used to select the speciation model.

Table 4. Composition, notation and formation constants (β) for the $\text{Cd}^{2+}/\text{cnge (L)}/\text{H}^+$ system (0.150 mol L^{-1} NaCl, 298 K).

Species (pqr)	Formula	$\log \beta$
011	LH	11.570
10-1	$[\text{CdH}_{-1}]^{1+}$	-9.650
102	$[\text{CdH}_{-2}]$	-19.800
11-3	$[\text{CdLH}_{-3}]^{2-}$	-20.630
210	$[\text{Cd}_2\text{L}]^{3+}$	15.590
121	$[\text{CdL}_2\text{H}]^{1+}$	24.440

Table 5. Composition, notation, and formation constants (β) for the $\text{Cd}^{2+}/\text{o-phen (A)}/\text{cnge (L)}/\text{H}^+$ system (0.150 mol L^{-1} NaCl, 298 K).

Species ($pqrst$)	Formula	$\log \beta$
0011	LH	11.570
0101	A	4.960
1100	$[\text{CdA}]^{2+}$	5.550
1200	$[\text{CdA}_2]^{2+}$	10.400
101-3	$[\text{CdLH}_{-3}]^{2-}$	-20.640
1021	$[\text{CdL}_2\text{H}]^{1+}$	24.440
2010	$[\text{Cd}_2\text{L}]^{3+}$	15.590
1111	$[\text{CdALH}]^{2+}$	23.140
1210	$[\text{CdA}_2\text{L}]^{1+}$	25.070
121-1	$[\text{CdA}_2\text{LH}_{-1}]$	15.570
1110	$[\text{CdAL}]^+$	11.330

The results obtained for the $\text{Cd}^{2+}/\text{phen}/\text{H}^+$ system were in agreement with data previously reported [17].

The ternary $\text{Cd}^{2+}/\text{cngeH}/\text{H}^+$ system shows a competition between free Cd and $[\text{Cd}_2\text{L}]^{3+}$ species up to pH 6.5 where the binuclear complex became the major species (figure 3, table 4). At pH values near 9, ca 40% of the $[\text{CdL}_2\text{H}]^+$ species forms, a percent that decreases at pH 10 when formation of hydroxo species ($[\text{CdLH}_{-3}]^{2-}$) occurs.

Several models for the $\text{Cd}^{2+}/\text{phen}/\text{cngeH}/\text{H}^+$ equilibrium have been tested in this work, based on ternary species. The proposed model for the quaternary system and the corresponding β values for the species are shown in table 5. The species distribution diagrams as a function of pH from 2 to 11 were obtained with the SPECIES program. The behavior of this system is described in the distribution species diagram of figure 4. At low pH the formation of the $[\text{CdALH}]^{2+}$ ($\log\beta_{1111} = 23.14$) is observed. At pH values above 3 a new species, $[\text{CdA}_2\text{L}]^+$, appears and remains as the major species in the pH range 4-9. Because of loss of protons, for pH values higher than 9 $[\text{CdA}_2\text{LH}_{-1}]$ ($\log\beta_{121-1} = 15.57$) prevails.

3.6. Antibacterial activity

The antibacterial activities of the complex and its components were explored by determining the zone of inhibition (discs diffusion tests) using gentamicin and ampicillin

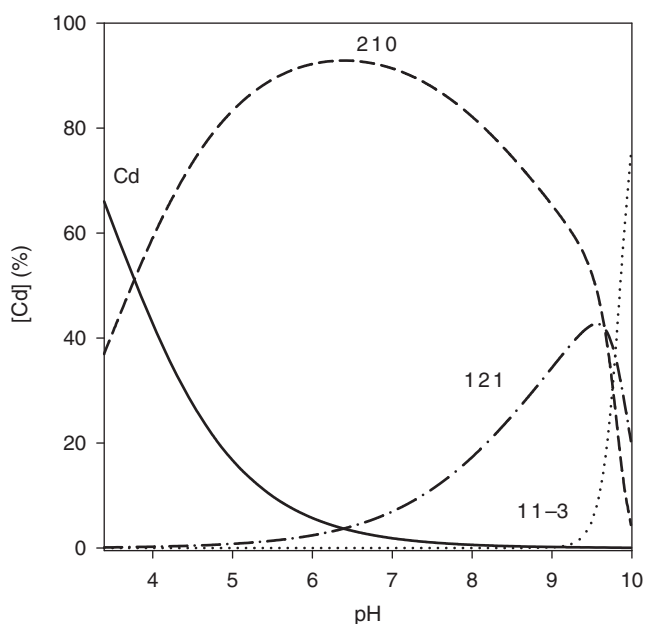


Figure 3. Species distribution for the $\text{Cd}^{2+}/\text{cnge (L)}/\text{H}^+$ system. Total concentrations: Cd^{2+} , 0.1 mmol L^{-1} and cnge, 0.2 mmol L^{-1} as a function of pH, 25°C , $I=0.150 \text{ mol L}^{-1}$ NaCl.

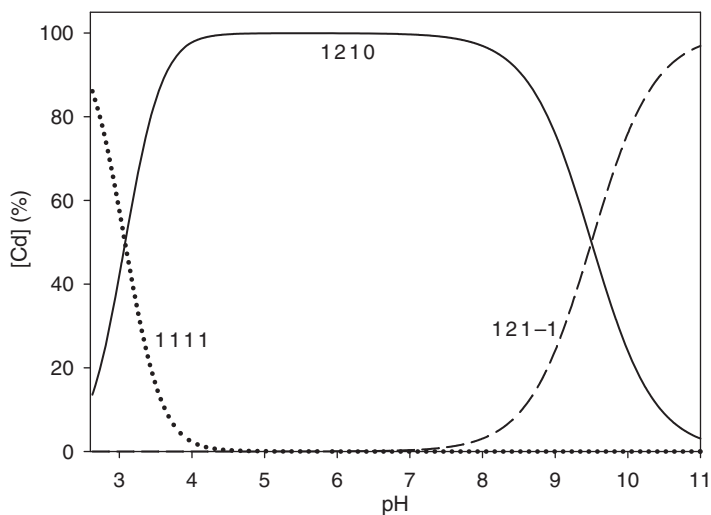


Figure 4. Species distribution for the $\text{Cd}^{2+}/\text{o-phen (A)}/\text{cnge (L)}/\text{H}^+$ system. Total concentrations: Cd^{2+} , 0.5 mmol L^{-1} , phen, 1.5 mmol L^{-1} and cnge, 1 mmol L^{-1} as a function of pH, 25°C , $I=0.150 \text{ mol L}^{-1}$ NaCl.

as reference standards (table 6). The antibiotic sensitivity profiles of bacterial strains show antibacterial activity for cadmium, phenanthroline, and the complex against Gram negative (*E. coli* and *P. aeruginosa*) and Gram positive (*S. aureus* and *E. faecalis*) microorganisms, as observed by the diameter of the diffusion.

Table 6. Antibiotic sensitivity profile of bacteria against cadmium, ortho-phenanthroline, cyanoguanidine, and the ternary complex, Cd²⁺/phen/cngeH in solution. Zone of inhibition (diameter in mm).

	<i>E. coli</i> ATCC 35218	<i>S. aureus</i> ATCC 25923	<i>P. aeruginosa</i> ATCC 27853	<i>E. faecalis</i> ATCC 29212
CdCl ₂	20.3 ± 0.6	22.2 ± 0.2	11.3 ± 0.6	18.7 ± 0.6
phenH	33 ± 1	34 ± 1	12.3 ± 0.6	21 ± 1
Cnge	0	0	0	0
Cd/phen/cnge 1 : 2 : 1	23.3 ± 0.6	25 ± 1	25.3 ± 0.6	23.3 ± 0.6
Gentamicin	23 ± 1	24.6 ± 0.6	24.6 ± 0.6	
Ampicillin				21 ± 1

Commercial gentamicin and ampicillin (positive controls) were used as supplied. When 0.27 μmol of cadmium was tested no effect was observed for the four strains (data not shown). To obtain a similar value of the positive standard of the complex, 0.4 μmol of each component were added to the discs.

All of the tested compounds were highly effective against *S. aureus*. The repressive effect of cadmium on growth in the tested microorganisms and the greater effect for *S. aureus* than for *E. coli* have previously been shown [34]. For *P. aeruginosa*, the metal antibacterial activity is less significant.

The free ligands (phenanthroline and cyanoguanidine) and their mixed ligand complex (considering the major species in solution at pH 4–9 as [CdA₂L]⁺, see figure 4) showed variable *in vitro* antimicrobial activities against the tested strains (table 6). Cyanoguanidine did not exert any antibacterial activity against the tested microorganisms. Phenanthroline showed a higher effect than the control gentamicin for *E. coli* and *S. aureus* but not for *P. aeruginosa* and a similar effect was found for *E. faecalis* and its control ampicillin. The observed order of zone of inhibition: *S. aureus*, *E. coli* > *E. faecalis* > *P. aeruginosa* is consistent with previous determinations of the minimum inhibitory concentrations for phenanthroline [35]. For *P. aeruginosa* a considerable improvement of the antibacterial activity was observed by complex formation. On the other hand, for *E. coli* and *S. aureus*, phenanthroline showed greater activity than the complex and the antibiotic.

Chelation theory explains the increase of the antimicrobial activity of the complex related to that of the free ligand [36]. Besides, the metal-binding sites in the enzymes of microorganisms are blocked and the respiration of the cells synthesis of proteins is perturbed with a consequent inhibition of the growth of the microorganisms. The antibacterial effect of the metal complexes can be due to either killing the microbe or inhibiting multiplication of the microbe by blocking their active sites [37]. This inhibitory effect is observed upon coordination of several compounds to cadmium and other transition metals ions [38–41] and particularly, in the improvement of the cadmium inhibitory effect upon coordination observed herein against *P. aeruginosa* strain (table 6).

Phenanthroline and its derivatives are of interest due to their potential activity against cancer, and viral, bacterial, and fungal infections, and their interaction with DNA occurs by aromatic π stacking between base pairs [42]. Furthermore, by fluorescence spectroscopy it has been shown that coordination increased the conformational rigidity of phenanthroline (see above) so the π-delocalization of the ligand

may be higher than in the chelate complex. It has previously been stated that conformationally restricted compounds showed a significant decrease in biological activity compared with conformationally unrestricted analogs [43], and that the conformational flexibility of peptides confers more potent antibacterial activities [44, 45]. The theory of cell permeability (Overtone's concept) takes into account that the liposolubility of the compounds control the antimicrobial activities because the lipid membrane that surrounds the cell allows the passage of lipid-soluble materials [46]. As a consequence, the higher flexibility of phenanthroline with respect to its cadmium complex may be the reason of the higher critical factors (lipophilicity and penetration into the lipid membranes) that confers a more potent antibacterial activity to the uncoordinated ligand against *E. coli* and *S. aureus*. Similar results were obtained for platinum complexes [42].

4. Conclusion

A new Cd complex with phenanthroline and cyanoguanidine has been synthesized and characterized. The cadmium has an N_4O_2 core involving a sulfate and water. Even though cyanoguanidine does not coordinate in the solid state, its NH_2 is an H-bond donor in three $N-H \cdots O(\text{sulf})$ interactions. Different behavior is observed in aqueous solution, where direct interaction of cnge and Cd is detected by potentiometric studies. The use of different solvents in the preparation of the solid compound and in the experimental determinations in the liquid state may generate such effects. Formation of a solid neutral species is favored over anionic species using ethanol–water mixtures. The *in vitro* antibacterial activity of the synthesized complex has been studied using various bacterial strains. Cadmium complexation with nitrogen containing bases in biological fluids can enhance the inhibitory effect of the metal.

Supplementary material

Listings of atomic coordinates and equivalent isotropic displacement parameters (table S1), full bond distances, and angles (table S2), anisotropic atomic displacement parameters (table S3), hydrogen atoms positions (table S4), and H-bond distances and angles (table S5). A CIF file with details of the crystal structure reported in this article has been deposited with the Cambridge Crystallographic Data Centre, under deposition number CCDC 821730.

Acknowledgments

This work was supported by UNLP, UNCAUS, CONICET (PIP1125 and PIP 1529), ANPCyT (PICT 2008-2218), CICPBA, and FAPESP (Brazil). EF, SBE, and OEP are members of the Carrera del Investigador, CONICET. PAMW is a member of the

Carrera del Investigador CICPBA, Argentina. MSI is a fellowship holder from CONICET.

References

- [1] A.T. Tan, R.C. Woodworth. *Biochemistry*, **8**, 3711 (1969).
- [2] D.L. Hamilton, L.S. Valberg. *Am. J. Physiol.*, **227**, 1033 (1974).
- [3] Z.S. Yang, J.S. Yu, H.Y. Chen. *Chin. J. Inorg. Chem.*, **18**, 373 (2002).
- [4] R.B. Gómez-Coca, L.E. Kapinos, A. Holý, R.A. Vilaplana, F. Gonzaez-Vilchez, H. Sigel. *J. Biol. Inorg. Chem.*, **9**, 961 (2004).
- [5] N.A. Illán-Cabeza, S.B. Jiménez-Pulido, J.M. Martínez-Martos, M.J. Ramírez-Expósito, M.N. Moreno-Carretero. *J. Inorg. Biochem.*, **103**, 1176 (2009).
- [6] J.M. Pérez, V. Cerrillo, A.I. Matesanz, J.M. Millán, P. Navarro, C. Alonso, P. Souza. *ChemBiochem.*, **2**, 119 (2001).
- [7] F. Shaheen, A. Badshah, M. Gielen, M. Dusek, K. Fejfarova, D. de Vos, B. Mirza. *J. Organomet. Chem.*, **692**, 3019 (2007).
- [8] M.K. Rauf, I. Din, A. Badshah, M. Gielen, M. Ebihara, D. de Vos, S. Ahmed. *J. Inorg. Biochem.*, **103**, 1135 (2009).
- [9] M. Cavicchioli, A.C. Massabni, T.A. Heinrich, C.M. Costa-Neto, E.P. Abrão, B.A.L. Fonseca, E.E. Castellano, P.P. Corbi, W.R. Lustrì, C.Q.F. Leite. *J. Inorg. Biochem.*, **104**, 533 (2010).
- [10] Enraf-Nonius. *COLLECT. B.V. Nonius*, Delft, The Netherlands (1997–2000).
- [11] Z. Otwinowski, W. Minor. In *Methods in Enzymology*, C.W. Carter Jr, R.M. Sweet (Eds), Vol. 276, pp. 307–326, Academic Press, New York (1997).
- [12] G.M. Sheldrick. *SHELXS-97, Program for Crystal Structure Resolution*, University of Göttingen, Göttingen, Germany (1997).
- [13] G.M. Sheldrick. *SHELXL-97, Program for Crystal Structures Analysis*, University of Göttingen, Göttingen, Germany (1997).
- [14] G. Gran. *Analyst*, **77**, 661 (1952).
- [15] E.G. Ferrer, L.L. López Têvez, N. Baeza, M.J. Correa, N. Okulik, L. Lezama, T. Rojo, E.E. Castellano, O.E. Piro, P.A.M. Williams. *J. Inorg. Biochem.*, **101**, 741 (2007).
- [16] J.M. Dale, C.V. Banks. *Inorg. Chem.*, **2**, 591 (1963).
- [17] M.J. Fahsell, C.V. Banks. *J. Am. Chem. Soc.*, **88**, 878 (1966).
- [18] G. Anderegg. *Helv. Chim. Acta*, **263-264**, 2397 (1963).
- [19] S. Canepari, V. Carunchi, P. Castellano, A. Messina. *Talanta*, **47**, 1077 (1998).
- [20] C.K. Johnson. *ORTEP-II. A Fortran Thermal-Ellipsoid Plot Program, Report ORNL-5318*, Oak Ridge National Laboratory, Tennessee, USA (1976).
- [21] H. Wang, R.G. Xiong, H.Y. Chen, X.Y. Huang, X.Z. You. *Acta Cryst.*, **C52**, 1658 (1996).
- [22] Y.H. Sun, Z.Y. Du, S.Y. Zhang, Y.F. He, Z.G. Zhou. *Acta Cryst.*, **C66**, m104 (2010).
- [23] L. Ye, J.W. Ye, K.Q. Ye, Y. Wang. *Acta Cryst.*, **63**, m75 (2007).
- [24] R.G. Xiong, C.M. Liu, D.G. Li, H. Wang, X.Z. You. *Polyhedron*, **16**, 1263 (1997).
- [25] F. Ramezanipour, H. Aghabozorg, S. Sheshmani, A. Moghimi, H. Stoeckli-Evans. *Acta Cryst.*, **E60**, m1803 (2004).
- [26] M. Harvey, S. Baggio, L. Suescunc, R.F. Baggio. *Acta Cryst.*, **C56**, 811 (2000).
- [27] R.B. Fahim, G.A. Kolta. *J. Phys. Chem.*, **74**, 2502 (1970).
- [28] L.A. Sheludyakova, E.V. Sobolev, L.I. Kozhevina. *J. Appl. Spectrosc.*, **55**, 661 (1991).
- [29] J.M. Alía, H.G.M. Edwards, F.J. García Navarro. *J. Mol. Struct.*, **597**, 49 (2001).
- [30] K. Nakamoto. *Infrared and Raman Spectra of Inorganic and Coordination Compounds*, 4th Edn, Wiley, New York (1986).
- [31] D.R. Xiao, Y.G. Li, E.B. Wang, L.L. Fan, H.Y. An, Z.M. Su, L. Xu. *Inorg. Chem.*, **46**, 4158 (2007).
- [32] D.M. Boghaei, F.B. Asl. *J. Coord. Chem.*, **60**, 1629 (2007).
- [33] A.E. Martell, R.J. Motekaitis. *Determination and Use of Stability Constants*, 2nd Edn, VCH, New York (1992).
- [34] J.J. Doyle, R.T. Marshall, W.H. Pfander. *Appl. Microbiol.*, **29**, 562 (1975).
- [35] S.B. Kalia, G. Kaushal, M. Kumar, S.S. Cameotra, A. Sharma, M.L. Verma, S.S. Kanwar. *Braz. J. Microbiol.*, **40**, 916 (2009).
- [36] R. Malhota, S. Kumar, K.S. Dhindsa. *Indian J. Chem.*, **32A**, 457 (1993).
- [37] N. Nishat, S. Hasnain, S. Dhyani Asma. *J. Coord. Chem.*, **63**, 3859 (2010).
- [38] S. Alghool. *J. Coord. Chem.*, **63**, 3322 (2010).
- [39] M. Klanithi, M. Rajarajan, P. Tharmaraj. *J. Coord. Chem.*, **64**, 842 (2011).

- [40] S. Sumathi, P. Tharmaraj, C.D. Sheela, R. Ebenezer, P.S. Bhava. *J. Coord. Chem.*, **64**, 1673 (2011).
- [41] S. Sumathi, P. Tharmaraj, C.D. Sheela, R. Ebenezer. *J. Coord. Chem.*, **64**, 1707 (2011).
- [42] S. Roy, K.D. Hagen, P.U. Maheswari, M. Lutz, A.L. Spek, J. Reedijk, G.P. van Wezel. *Chem. Med. Chem.*, **3**, 1427 (2008).
- [43] C.S. Cooper, M.D. Tufano, P.K. Donner, D.T.W. Chu. *Bioorg. Med. Chem.*, **4**, 1307 (1996).
- [44] D. Oh, S.Y. Shin, S. Lee, J.H. Kang, S.D. Kim, P.D. Ryu, K.S. Hahm, Y. Kim. *Biochemistry*, **39**, 11855 (2000).
- [45] S.A. Lee, Y.K. Kim, S.S. Lim, W.L. Zhu, H. Ko, S.Y. Shin, K.S. Hahm, Y. Kim. *Biochemistry*, **46**, 13653 (2007).
- [46] Y. Anjaneyulu, R.P. Rao. *Synth. React. Inorg. Met. Org. Chem.*, **16**, 257 (1986).

Copyright of Journal of Coordination Chemistry is the property of Taylor & Francis Ltd and its content may not be copied or emailed to multiple sites or posted to a listserv without the copyright holder's express written permission. However, users may print, download, or email articles for individual use.